

Dynamics of pedogenic carbonate growth in the monsoonal tropical domain

A. Licht^{1,2}, J. Kelson³, S. Bergel², A. Schauer², S.V. Petersen³, A. Capirala², K.W. Huntington², G. Dupont-Nivet^{4,5}, Zaw Win⁶, and Day Wa Aung⁷

¹Centre de Recherche et d'Enseignement de Géosciences de l'Environnement (CEREGE), CNRS and Aix-Marseille University, Aix-en-Provence, France

²Department of Earth and Space Sciences, University of Washington, Seattle, WA, USA

³Department of Earth and Environmental Sciences, University of Michigan, Ann Arbor, MI, USA

⁴Géosciences Rennes, CNRS and Université de Rennes 1, Rennes, France

⁵Institut für Geowissenschaften, Universität Potsdam, Potsdam, Germany

⁶Geology Department, Shwe Bo University, Sagaing Region, Myanmar

⁷Department of Geology, University of Yangon, Pyay Road, Yangon, Myanmar

Corresponding author: Alexis Licht (licht@cerege.fr)

Key Points:

- soil carbonates under tropical monsoonal climate grow in winter and early spring.
- This seasonal bias is favored by warm (>15°C) winter temperatures and sustained rainfall from mid spring to late fall.
- A cold season bias in clumped isotope temperatures constitutes a potential signature for past tropical monsoonal climate in paleosols.

Abstract:

Pedogenic carbonate is widespread at mid latitudes where combined warm and dry conditions favor soil carbonate growth from spring to fall. The mechanisms and tempo of pedogenic carbonate formation are more ambiguous in the tropics, where longer periods of soil water saturation and higher soil respiration enhance calcite dissolution. This paper provides bulk and clumped isotope values from Quaternary and Miocene pedogenic carbonates in the tropical monsoonal domain of Myanmar where annual rainfall reaches up to 1700 mm. We show that carbonate growth in Myanmar is delayed to the coldest months of the year by sustained rainfall from mid spring to late fall. We propose that high soil moisture year-round in the tropical domain makes carbonate growth more episodic than in temperate ecosystems, and particularly sensitive to the seasonal distribution of rainfall. This sensitivity is also enhanced by high winter temperatures, allowing carbonate growth to occur outside the warmest months of the year. This high sensitivity is expected to be more prominent in the geological record during times with higher temperatures and greater expansion of the tropical realm. The winter bias in TA_{47} values found in Burmese soils, unique for pedogenic carbonates, constitute a potential signature for past tropical monsoonal (warm summer-wet) climates in paleosols, and are also found in our Miocene samples.

Plain Language Summary

Soil carbonates are the focus of numerous paleoenvironmental studies because their isotopic composition records many features of the local environment (such as the type and density of vegetation, annual or warm season temperatures, and aridity). Soil carbonates are commonly studied in temperate and arid areas; in those environments, carbonates form during warm months when soils dry. Soil carbonates are rarer but present in the tropics, where they have been barely studied. This study provides stable isotopic data from soil carbonates in the tropical monsoonal domain of Myanmar. We show that these soil carbonates grow during the coldest months of the year and follow different dynamics and isotope systematics than those of temperate and arid areas. We show that high soil wetness and warm temperatures year-round make carbonate growth particularly sensitive to the seasonal distribution of rainfall in the tropical domain. This seasonal sensitivity complicates the interpretation of soil isotopic data from past tropical ecosystems. We suggest that isotopic data from tropical paleoenvironments can be used as a proxy to reconstruct past rainfall distribution instead of average (or summer) environmental features.

1. Introduction

Soil carbonates are widespread from low to high latitudes, today and in the sedimentary archives, making them a valuable record of paleoenvironmental change through geologic time (e.g. Quade et al., 2011; Caves et al., 2015; Page et al., 2019; Xiong et al., 2020). However, most studies that investigate the features and growth dynamics of modern pedogenic carbonates have focused on temperate and (semi-)arid soils at mid latitudes, where calcic soils are abundant (e.g. Kelson et al., 2020). The dynamics of carbonate growth in the tropics remain barely explored, and it is unclear when and how tropical carbonates grow.

Soil carbonate grows in soils where Ca^{2+} is available and usually accumulates through multiple events of precipitation and dissolution that are controlled by soil water content, temperature, and CO_2 concentration (Breecker et al., 2009; Huth et al., 2019). Carbonate precipitation is favored during warm and dry times because high soil temperatures decrease calcite solubility while evaporation increases calcium activity in the soil water (Gallagher and Sheldon, 2016; Fischer-Femal and Bowen, 2021). By contrast, carbonate dissolution is favored during wetter periods, especially during the plant growing season with high soil respiration and soil CO_2 maxima (Breecker et al., 2009). Soil carbonate growth temperatures reconstructed using clumped isotope thermometry (TA_{47}) commonly show higher values than the Mean Annual Temperature (MAT) in temperate and (semi-)arid ecosystems, supporting a warm-season bias in carbonate growth (Kelson et al., 2020). This warm bias relative to mean annual air temperatures is sometimes enhanced in arid and semi-arid environments (with commonly < 500 mm of annual rainfall): solar heating increases summer soil temperatures relative to air temperature where soil surface is bare, while winter snow cover can mute winter soil temperatures (Gallagher et al., 2019).

Pedogenic carbonates are rarer at low latitudes but can be found in tropical seasonal areas (areas with average monthly temperatures above 18°C and at least one month with less than 60 mm of rainfall, sensu the Köppen classification), including close to the equator (Bettis et al., 2009). The mechanisms favoring soil carbonate formation and preservation in these warmer and wetter ecosystems are currently unclear given that higher soil respiration and longer periods of soil water saturation in tropical areas promote carbonate dissolution. In particular, the warm-season bias for carbonate growth may be less likely in the tropical monsoonal domain as warm temperatures in the late spring and summer are associated with intense rainfall, soil water saturation, and high soil respiration. In some regions with high summer rainfall outside the tropical domain, the carbonate growth season is delayed towards the fall such as in the Andes (Peters et al., 2013), but other regions such as Tibet do not show the same pattern (Quade et al., 2013; Burgener et al., 2018). A summer season bias for pedogenic carbonate growth remains the assumption of most studies using bulk and clumped isotope proxies on paleosols, including in the Asian monsoonal domain (Quade et al., 2011; Hoke et al., 2014; Ingalls et al., 2018; Botsyun et al., 2019; Xiong et al., 2020). This assumption is yet to be validated by a systematic study of soil carbonate growth in the tropics.

We address this discrepancy by providing an expanded dataset of bulk and clumped isotope values from Quaternary and Miocene soil carbonates in the tropical monsoonal domain of Myanmar, at sites where annual rainfall currently spans from 600 to 1700 mm. Our clumped and stable isotopic data indicate that carbonate growth varies locally from early winter to early spring. We explore the mechanisms leading to these cold TA_{47} values, unique so far in pedogenic carbonates, and highlight that soil carbonates grown under tropical climate follow different clumped and stable isotope systematics from their temperate and arid counterparts.

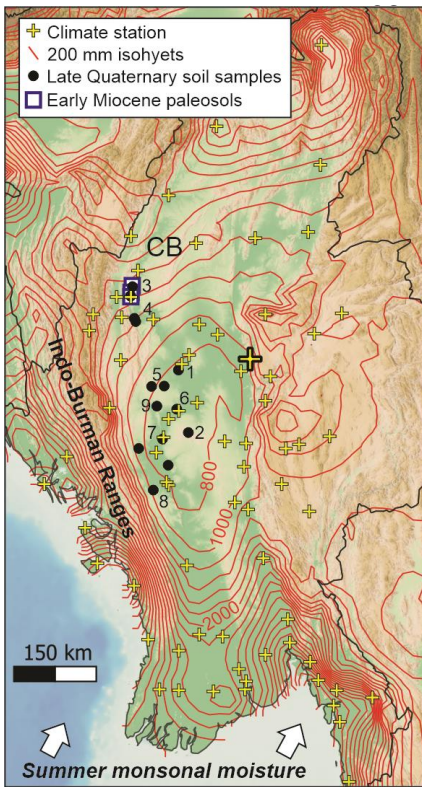


Figure 1. Map of western and central Myanmar with 200 mm isohyets of annual rainfall (red lines), Burmese climate stations (yellow crosses), Quaternary soil samples (black dots) and early Miocene paleosols (blue squares); numbers from 1 to 9 refer to sample location in Table 1. The location of the Mandalay climate station (Fig. 2a) is indicated with a bold cross. CB: Chindwin Basin.

2. Climate setting

Myanmar sits today in the South Asian monsoonal domain. Western Myanmar experiences intense summer rainfall (2-4 m from May to November) sourced from the Indian Ocean and amplified by the orographic effect of the Indo-Burman Ranges. Lying in the rainshadow of the ranges, the central Myanmar lowlands are located near sea-level and experience dramatic changes of Mean Annual Precipitation (MAP) over short distances, from 4 m in southern Myanmar to 600 mm in the “dry belt” of central Myanmar (Fig. 1). In contrast, the lowlands experience little regional temperature variation in monthly

107

108 temperatures ($\pm 3^\circ\text{C}$ of variation among climate stations). Mean Annual Temperature (MAT) ranges from 23
 109 to 28°C ; winter monthly temperatures average 17 to 22°C , with minima of $10\text{--}15^\circ\text{C}$; average monthly
 110 temperatures peak at $30\text{--}33^\circ\text{C}$ in April-May, with average monthly maxima of 40°C . Temperatures remain
 111 high (between 27 and 30°C) during the rainy season, which spans all summer and fall (Fig. 2a). The area is
 112 covered by mixed deciduous forests, woodlands, and savanna-woodlands. The vegetation is dominated by
 113 C3 trees and shrubs with limited herbaceous ground cover; C4 plants represent ca. 25% of the herbaceous
 114 vegetation (Khaing et al., 2019).

115 Unfortunately, there is no rainfall isotope data from the dry belt of central Myanmar. The closest station,
 116 Yangon, experiences more intense rainfall (> 2 m) and does not provide data outside the monsoon season
 117 (Fig. 2b); New Delhi, India, receives a relatively low amount of annual precipitation (ca. 800 mm, mostly in
 118 JJA) and is the closest GNIP station with a similar monsoonal climate to the Burmese dry belt. Both stations
 119 display increased isotopic depletion through the monsoonal season, reaching their lowest $\delta^{18}\text{O}$ values (-8 to $-$
 120 9 ‰ VSMOW) in September (New Delhi) and October (Yangon). Non-monsoonal rainfall (December to
 121 May) in New Delhi is much more ^{18}O -enriched: -3 to $+1$ ‰ VSMOW, similar to what is seen regionally in
 122 South Asia (Araguas-Araguas et al., 1998). Therefore, we estimate the isotopic composition of rainfall in our
 123 study region to follow a similar seasonal pattern.

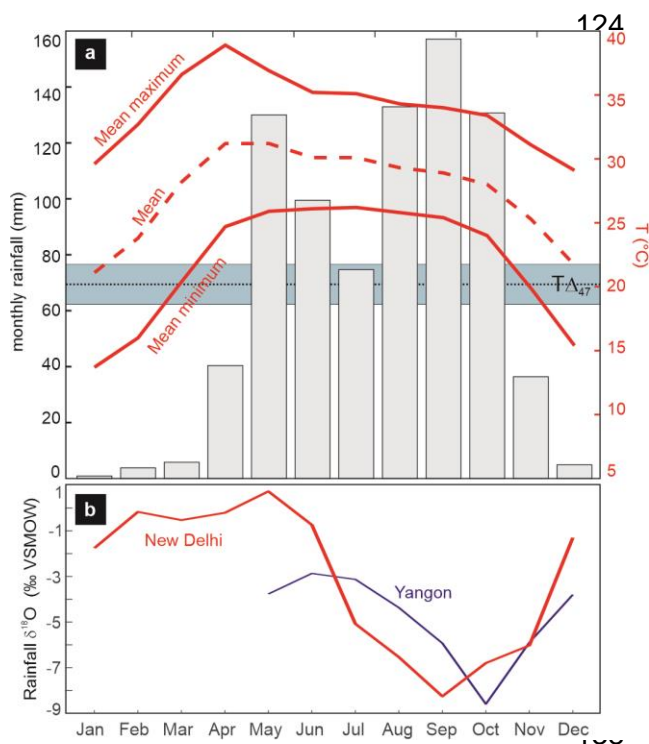


Figure 2. (a) Mean, mean maximum, and mean minimum monthly air temperatures (in red) and mean monthly precipitation (bars) in Mandalay (MAT: 27°C; MAP: 891 mm), displayed with the weighted average $T\Delta_{47}$ and standard error (2 SE) of all Burmese samples (in green). Mean temperature data are from the global historical climatology network monthly temperature dataset, version 4 (Menne et al., 2018); temperature maxima, minima, and rainfall data from Lai Lai Aung et al. (2017); all climatic data are also available in Supplementary Table 1. (b) Monthly rainfall $\delta^{18}O$ in Yangon and New Delhi; data from the Global Network of Isotopes in Precipitation (GNIP); only May to December data are available in Yangon.

3. Methods

Our field investigations in central Myanmar show that pedogenic carbonates are widespread in the central dry belt and can be found in areas with up to 1.7 m of annual rainfall. We collected pedogenic carbonates from 15 localities along road cuts and badlands, in poorly developed soils (inceptisols) to ensure their young age. Three localities are soils developed on recent, loose river alluvium (including one on former farmland), and one locality on Mount Popa volcanoclastics attributed to the early Holocene (Belousov et al., 2018). The other localities are soils developed on tilted Eocene, Miocene and Pliocene sedimentary rocks; considering the recent deformation history of the central Myanmar lowlands (Plio-Pleistocene; Pivnik et al., 1998) and the current high denudation rates in the central dry belt during the monsoon season (Stamp, 1940), these soils are attributed to the Quaternary. Seasonal temperatures and rainfall amount at the 15 localities were obtained from three sources: 1) outputs from the WorldClim 2.1 model at 5 minutes spatial resolution (Fick and Hijmans, 2017); 2) variables from the closest climate station in central Myanmar (for monthly temperature maxima, minima, and rainfall amount; Fig. 1); and 3) variables at the locality extrapolated from Burmese climate stations with triangle-based cubic interpolation. The three approaches yield very similar results for monthly and annual variables (Supplementary Table 1).

Carbonate nodules were sampled at depths greater than 50 cm; up to five nodules per locality were selected for $\delta^{18}O$ and $\delta^{13}C$ analysis; samples were powdered and analyzed on a Kiel III Carbonate Device coupled to a Finnigan Delta Plus isotope ratio mass spectrometer at the University of Washington. Clumped isotope analysis was performed on one to two carbonate samples from ten of the localities, with 4-11 replicates each; ten samples were analyzed at the University of Washington (digestion in a common acid held at 90 °C, purification on an off-line vacuum system, and analysis on a MAT 253, following Kelson et al., 2017) and at

the University of Michigan (digestion and purification in a NuCarb automated sample preparation device held at 70 °C, and analysis on a Nu Perspective). The resulting Δ_{47} values are standardized to the InterCarb framework (Bernasconi et al., 2021) and are converted to clumped isotope temperatures ($T\Delta_{47}$, in °C) following Anderson et al. (2021). Soil water $\delta^{18}\text{O}$ is then calculated from carbonate $T\Delta_{47}$ and $\delta^{18}\text{O}$ values using the equation of Kim and O'Neil (1997).

We calculated soil CO_2 $\delta^{13}\text{C}$ isotopic composition at each site from their average carbonate $\delta^{13}\text{C}$ value, using the T-dependent fractionation equation of Romanek et al. (1992) and an estimate of soil temperature during carbonate growth. These estimates were obtained from either the $T\Delta_{47}$ value at the site, the average $T\Delta_{47}$ value if two measurements were made at the site, or the average $T\Delta_{47}$ value at all localities (20.1 °C; cf next section) if no clumped isotopic data were acquired. Finally, for eleven of the localities, we acquired solid organic matter $\delta^{13}\text{C}$ values from decarbonated material from the carbonate layers. Solid samples were left overnight with 6M HCl in an oven at 60-80°C and rinsed with DI water the following day, and thus for three consecutive days; $\delta^{13}\text{C}$ values of decarbonated material were acquired with a Costech Elemental Analyzer, Conflo III, MAT253 in continuous flow mode at the University of Washington.

We also sampled pedogenic nodules from the upper lower Miocene to lowermost middle Miocene Natma Formation in the Chindwin Basin, close to our wettest localities (modern MAP: ca. 1700 mm; Fig. 1). The Natma Formation consists of fluvial deposits rich in paleosols (mostly cumulative argillisols and rare argillic calcisols) and fossil wood specimens typical of moist deciduous to (semi-)evergreen forests found in monsoonal Southeast Asia (Gentis et al., 2019; Westerweel et al., 2020). Thirty samples from seven localities were prepared in thin section and examined using polarized light microscopy to evaluate the absence of secondary, sparitic calcite. Nineteen of these pedogenic carbonate samples were analyzed for carbon and oxygen isotopes; two samples were almost devoid of sparite and selected for clumped isotope analysis at the University of Washington (microphotographs of thin sections available in Supplementary File 1). We also acquired solid organic material $\delta^{13}\text{C}$ values from decarbonated material of the carbonate layers for four of the localities.

Location of samples, soil and paleosol details (sampling depth, soil texture and vegetation cover), and climate variables at the site and at the nearest climate stations are given in Supplementary Table 1; a synthesis of clumped isotope data is provided in Table 1; detailed bulk and clumped isotope results together with analytical procedures are given in Supplementary Table 2, and microphotographs of thin sections in Supplementary file 1. Raw clumped isotopic data from the University of Washington and University of Michigan are given in Supplementary Tables 3 and 4.

4. Results

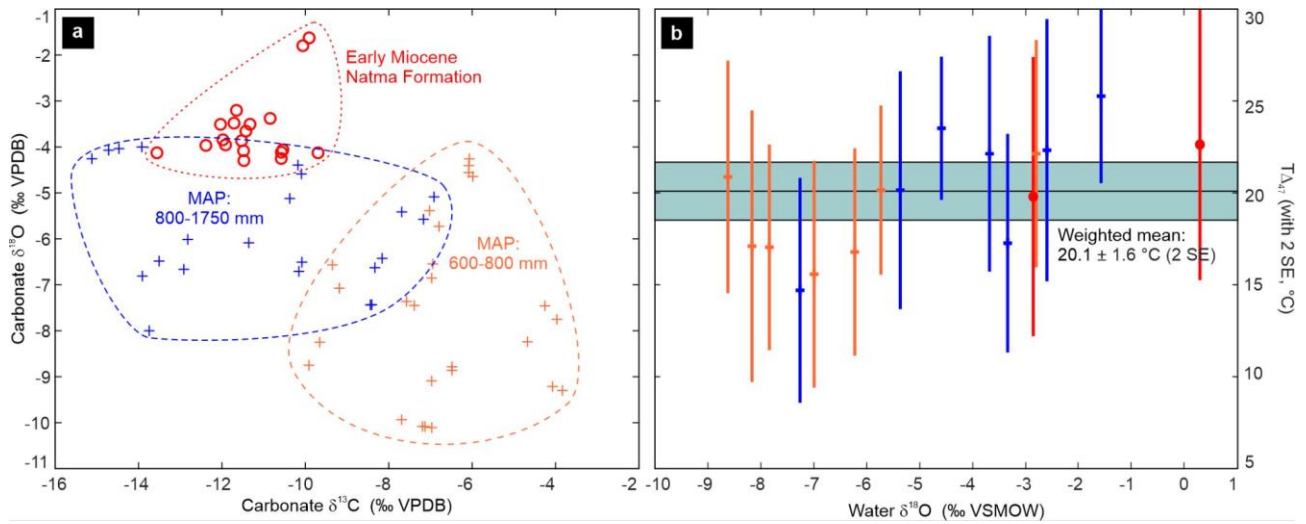


Figure 3. (a) Oxygen and carbon isotopic composition of pedogenic carbonates from central Myanmar.

Quaternary samples (crosses) are sorted following the MAP at their locality: 600-800 mm (in orange), 800-1750 mm (in blue); early Miocene samples (circles) are displayed in red. **(b)** $T\Delta_{47}$ values and water $\delta^{18}\text{O}$ values of pedogenic carbonates from central Myanmar (color coding same as in a); the weighted mean and weighted standard error (2 SE) for quaternary samples is displayed in gray. Error bars for $T\Delta_{47}$ values are 2 SE of replicate analyses. Propagated $T\Delta_{47}$ error in water $\delta^{18}\text{O}$ values (always <0.8 ‰ at 1 SE) is not shown for simplicity.

We split the dataset of Quaternary carbonates into two climatic groups of even size for a balanced comparison: samples from localities below and above 800 mm MAP. Localities with MAP below 800 mm (7 localities, 26 stable isotopic and 7 clumped isotopic data points) cover a wide range of carbonate $\delta^{18}\text{O}$ values: from -4 to -10 ‰ VPDB, with an average of -7.6 ‰ (Fig. 3a). Carbonate $\delta^{13}\text{C}$ values range between -3 and -10 ‰ VPDB (average: -6.7 ‰). $T\Delta_{47}$ values range from 15 ± 6 °C to 22 ± 6 °C (2 SE), with a weighted average and standard error of 18.7 ± 2.2 °C (2 SE; Fig. 3b). Water $\delta^{18}\text{O}$ values reconstructed from $T\Delta_{47}$ and carbonate $\delta^{18}\text{O}$ values range from -3 to -9 ‰ VSMOW (average -6.6 ‰). In contrast, localities with MAP above 800 mm (8 localities, 22 stable isotopic and 7 clumped isotopic data points) display more enriched $\delta^{18}\text{O}$ values, spanning from -4 to -8 ‰ VPDB, with an average at -5.8 ‰. Carbonate $\delta^{13}\text{C}$ values are much more depleted, from -7 to -14 ‰ VPDB (average: -11.0 ‰). $T\Delta_{47}$ values range from 15 ± 6 °C to 25 ± 5 °C (2 SE), with a weighted average and standard error of 21.4 ± 2.1 °C (2 SE). Water $\delta^{18}\text{O}$ values reconstructed from $T\Delta_{47}$ values range from -2 to -7 ‰ VSMOW (average -4.0 ‰). The weighted average $T\Delta_{47}$ value of both groups remains close to the weighted average of the complete population (20.1 ± 1.6 °C, 2 SE). Interestingly, samples with low water $\delta^{18}\text{O}$ values are almost systematically associated with lower-than-average $T\Delta_{47}$ values, while samples with high water $\delta^{18}\text{O}$ values are associated with the warmest temperatures. Carbonates with $\delta^{18}\text{O}$ values below -6 ‰ VSMOW (6 samples) have an average $T\Delta_{47}$ value of 16.9 ± 2.5 °C (2 SE), while less depleted samples (8 samples) have an average $T\Delta_{47}$ value of 22.0 ± 1.9 °C (2 SE). Finally, soil organic matter sampled in the carbonate layers at eleven localities displays $\delta^{13}\text{C}$ values ranging from -27 to -22 ‰ VPDB (Fig. 4), with no clear difference between groups. These values are typical

of the $\delta^{13}\text{C}$ range for C3 flora outside tropical rainforests (Kohn, 2010), but do not reject a potential presence of a small proportion of C4 plants (<20 %).

Samples from the Miocene Natma Formation (7 localities, 19 stable isotopic and 2 clumped isotopic data points) display carbonate $\delta^{18}\text{O}$ values between -3 to -5 ‰ VPDB (average: -3.6 ‰), with the exception of one locality that displays more enriched values (between -1 and -2 ‰). Carbonate $\delta^{13}\text{C}$ values range from -9 to -14 ‰ VPDB (average: -11.3 ‰). $T\Delta_{47}$ values equal $20 \pm 8^\circ\text{C}$ and $23 \pm 6^\circ\text{C}$ (2 SE), with reconstructed water $\delta^{18}\text{O}$ values from -3 to 0 ‰ VSMOW. Lastly, soil organic matter at four localities displays $\delta^{13}\text{C}$ values ranging from -26 to -24 ‰ VPDB, again typical of C3 flora outside tropical rainforests (Fig. 4).

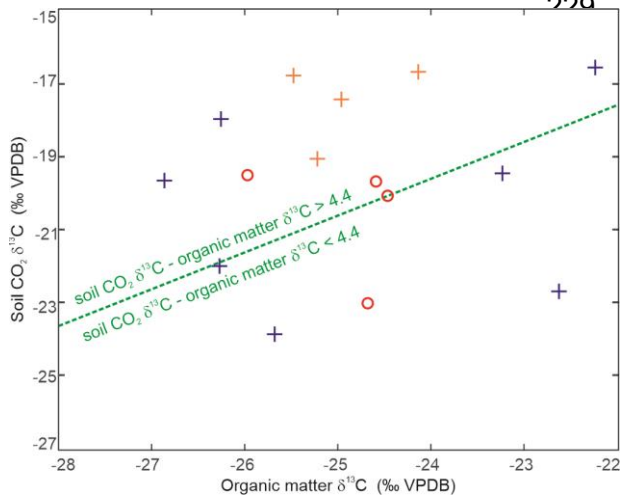


Figure 4. Organic matter $\delta^{13}\text{C}$ values for the Quaternary and Miocene localities, compared to their calculated soil CO_2 $\delta^{13}\text{C}$ values (see main text). Color coding is the same as Figure 3: Quaternary samples at localities with MAP < 800 mm (orange crosses), > 800 mm (blue crosses), and Miocene samples (red circles). The dashed green line highlights the domain where soil CO_2 $\delta^{13}\text{C}$ = organic matter $\delta^{13}\text{C}$ + 4.4 ‰, the minimum fractionation observed if soil carbonates and organic matter are contemporaneous (Cerling et al., 1991; Montanez, 2013).

Localities			Climate parameters from WorldClim V2, res 5min				Clumped isotopic data									
age	location on fig. 1	name	MAT (in °C)	WMMT (in °C)	CMMT (in °C)	MAP (in mm)	<i>n</i>	Carbonate $\delta^{13}\text{C}$ (‰ VPDB)	$\delta^{13}\text{C}$ S.E. (‰ VPDB)	Carbonate $\delta^{18}\text{O}$ (‰ VPDB)	$\delta^{18}\text{O}$ S.E. (‰ VPDB)	Δ_{47} Intercarb acid (‰)	Δ_{47} S.E. (‰)	$T\Delta_{47}$ (°C)	$T\Delta_{47}$ S.E. (°C)	Soil Water $\delta^{18}\text{O}$ (‰ VSMOW)
Quaternary soils	1	17NOD01	27.2	31.3	21.2	747	8	-6.08	0.02	-4.56	0.16	0.6904	0.0092	22.1	3.0	-2.8
	2	17NOD04	25.1	29.6	19.9	772	11	-6.97	0.04	-10.11	0.02	0.6943	0.0099	20.9	3.2	-8.6
	3	19NOD02	24.3	28.5	18.1	1701	6	-10.18	0.02	-4.39	0.03	0.6898	0.0107	22.3	3.5	-2.6
	3	19NOD03	24.3	28.5	18.1	1701	7	-10.16	0.03	-6.71	0.07	0.6965	0.0099	20.2	3.1	-5.3
	4	19NOD04	25.7	29.8	19.5	1372	9	-14.72	0.01	-4.07	0.03	0.7056	0.0097	17.3	3.0	-3.3
							4	-13.92	0.01	-4.00	0.02	0.6806	0.0073	25.4	2.4	-1.5
	5	19NOD06	25.7	30.0	20.0	845	7	-8.44	0.02	-7.44	0.03	0.7140	0.0099	14.7	3.0	-7.2
							6	-8.33	0.01	-6.63	0.07	0.6862	0.0059	23.5	2.0	-4.6
	6	19NOD07	27.6	31.9	22.1	647	10	-6.97	0.01	-6.85	0.03	0.7072	0.0092	16.8	2.8	-6.2
	5	19NOD08	27	31.3	21.3	720	10	-6.48	0.02	-8.86	0.13	0.7061	0.0121	17.1	3.7	-8.1
	7	19NOD09	27.3	31.6	21.9	655	7	-7.57	0.06	-7.36	0.07	0.7111	0.0099	15.6	3.0	-7.0
	8	20NOD01	27	31.5	20.9	869	7	-7.70	0.09	-5.43	0.07	0.0096	0.0099	22.2	3.2	-3.6
9	20NOD03	26.8	31.0	21.4	723	8	-9.89	0.02	-8.59	0.06	0.7063	0.0093	17.1	2.9	-7.9	
						4	-9.19	0.01	-7.07	0.03	0.6965	0.0073	20.2	2.3	-5.7	
Early Miocene	3	19NAT13	N/A				8	-9.70	0.48	-4.13	0.90	0.6976	0.0121	19.8	3.8	-2.8
	3	19NAT01	N/A				5	-9.91	0.06	-1.63	0.05	0.6881	0.0091	22.9	3.0	0.3

240

Table 1. Synthesis of clumped isotope data and soil water $\delta^{18}\text{O}$ at each locality; climatic parameters from

241

Worldclim V2 at 5 minutes resolution; alternate climate parameters and soil morphology at every locality described in Supplementary Table 1, detailed clumped isotope data in supplementary Table 2. n = number of replicates; $T\Delta_{47}$ values are calculated with a temperature- Δ_{47} relationship of Anderson et al. (2021). Soil water $\delta^{18}\text{O}$ values are calculated from carbonate $\delta^{18}\text{O}$ and $T\Delta_{47}$ values using the equation of Kim and O'Neil (1997). Propagated $T\Delta_{47}$ error in water $\delta^{18}\text{O}$ values range from 0.8 to 1.6 ‰ (2 SE).

5. Discussion

5.1 A record of multiple glacial and interglacial periods?

The average $T\Delta_{47}$ value (20.1 ± 1.6 °C, 2 SE) is only reached today in central Myanmar during winter (DJF; Fig. 1). The $T\Delta_{47}$ values of some individual sites are colder on average than winter temperatures (15 ± 6 °C, 2 SE), but still overlap with the Coldest Month Mean Temperature (CMMT) at the study sites (17-22 °C). This misfit suggests that these soil carbonates formed, or partially formed, during colder periods of the Quaternary.

Carbon isotopic data also support the idea that some of the soil carbonates at the wetter sites might have formed at least partially during an earlier period or might integrate over a longer period of time (> several millennia) with varying environmental conditions. Soil CO_2 has a carbon isotopic composition at least 4.4-4.2 ‰ higher than soil organic matter due to differences in diffusion between different CO_2 isotopologues during soil respiration (Cerling et al., 1991). Differences lower than 4.4-4.2 ‰ are commonly explained as related to recent changes in soil organic matter because labile organic matter has a faster turnover rate than pedogenic carbonate growth (Montanez, 2013). Of the wet sites (MAP > 800 mm) for which we have $\delta^{13}\text{C}$ values of organic matter, more than half (4 out of 7) display soil CO_2 $\delta^{13}\text{C}$ values that are less than 4.4 ‰ higher than those of the soil organic matter (Fig. 4). These results indicate that carbonates at the wettest sites grew partly (or completely) from soil-respired CO_2 and organic matter that was more ^{13}C -depleted than currently, which supports an earlier origin for some of our samples. Plant carbon isotopic composition in monsoonal (sub)tropical forests mainly relates to habitat openness, with lowest $\delta^{13}\text{C}$ values in areas with the lowest light availability (Ehleringer et al., 1987). At a broader spatial scale, plant carbon isotopic composition in C3 plant communities is linked to humidity, with lowest $\delta^{13}\text{C}$ values in the wettest areas (Kohn, 2010). Therefore, more depleted soil-respired CO_2 at the time of carbonate formation at the wettest sites indicates that these carbonates grew at least partially under denser forest cover than is present today, and possibly wetter conditions.

Surface temperatures were ca. 2-5°C lower in South Asia during the last glacial maximum (Saraswat et al., 2013; Liu et al., 2020); partial carbonate growth during previous glacial periods could thus explain the colder-than-winter values found in some of our samples. However, it is difficult to assess if the more forested and possibly wetter conditions do indeed correspond to the last glacial periods, as the past hydrological history of Myanmar is poorly understood. Climate simulations suggest an increase of annual rainfall over the Indo-Burman Ranges and western Myanmar during the last glacial period (Di Nezio et al., 2018), corroborated by higher erosion rates in the ranges (Colin et al., 2001). In contrast, speleothems in eastern

Myanmar (Shan-Thai Highlands) and Thailand suggest a ~60% decrease of monsoonal rainfall at that time (Liu et al., 2020). Human-mediated deforestation during the late Holocene also could have partly driven the observed discrepancy between carbonate and organic matter $\delta^{13}\text{C}$ values. The two pre-Quaternary samples analyzed here yield TA_{47} values (20 and 23 °C) similar to the weighted TA_{47} average of our Quaternary samples. The two soil localities unequivocally attributed to the Holocene (19NOD07, developed on former farmland, and 17NOD04, developed on early Holocene volcanoclastics) yield similar temperatures (17 and 21°C). This suggests that the integration of glacial temperatures in our Quaternary TA_{47} values is not the main driver lowering our carbonate growth temperature record to coolest average monthly temperatures. Even by decreasing monthly temperatures of modern air by 2 to 5 °C, as expected during the last glacial period in South Asia, the average TA_{47} temperature (20.1 ± 1.6 °C, 2 SE) remains within the range of monthly average temperatures during winter to early spring (December to April; e.g. Fig. 2a). Our TA_{47} values thus indicate a cold-season bias in carbonate growth, even when considering a potential integration of soil temperatures through multiple glacial and interglacial cycles.

5.2 Presence, mechanisms and timing of carbonate growth in the tropical domain

The presence of soil carbonate in some of the wettest parts of central Myanmar, and their growth during possibly wetter conditions, is contrary to the traditional wisdom that soil carbonates do not form in environments with $\text{MAP} > 1000$ mm/year (Retallack, 2005). While this occurrence is rare, soil carbonates have been observed in “wet” localities such as northern India (Singh and Singh, 1972) and Tennessee, USA (Railsback, 2021). Quaternary pedogenic nodules are also found in multiple localities near the equator in Java (latitude ca. 7°N), in areas with prominent seasonality and modern annual rainfall exceeding 1700 mm (van Der Kaars and Dam, 1997; Bettis et al., 2009). Following Breecker et al. (2009, 2010), we propose that the intensely seasonal nature of precipitation and soil water content in Myanmar allows for preferential formation of carbonates during the dry season, in winter and early spring.

The long monsoonal season in Myanmar, with intense and steady rainfall from May until October (Fig. 2a), results in a delayed peak of soil moisture in late Fall (mid November; Fig. 5). In winter and spring (December to May), central Myanmar experiences little rainfall and monthly temperatures remain above 15°C; these warm and dry conditions allow the soils to steadily dry until the onset of the next monsoon season. Pedogenic carbonates in this region are thus expected to form throughout the winter and spring, including through the spring months of April and May when monthly temperatures peak above 30°C, as soil drying continues to concentrate Ca^{2+} ions in the soil and promote saturation of calcite (Breecker et al., 2009). Our TA_{47} values do indeed indicate that carbonate growth occurs here in the winter and spring, but in contrast display an apparent bias towards the earlier part of the dry season. This bias could partly result from an imprint of glacial temperatures, or alternatively suggests a narrow period of carbonate growth at the start of the seasonal dewatering phase. Specifically, this apparent bias in temperatures could be a result of two processes: 1) soil respiration may increase enough in late spring to reduce calcite precipitation and/or 2) carbonate that forms in later spring may be more sensitive to dissolution than winter-grown carbonates, as described in the following paragraphs.

(1) Soil respiration is primarily controlled by soil moisture in Asian monsoonal ecosystems, with low values in the dry season and high values during the monsoon season (Kume et al., 2013, Hanpattanakit et al., 2015). Winter months in central Myanmar display the lowest monthly rainfall amount (commonly <10 mm per month from December to March; Fig. 2a). Sparse but heavy rain events during mid-spring (April-May) do not impact the average soil moisture budget (Fig. 5) but could result in rain-induced soil respiration pulses, as seen in other seasonal tropical forests (Rubio and Detto, 2017). These pulses of soil moisture and soil respiration could prevent spring carbonate growth. In addition to this important moisture control, temperature variations within the dry season sometimes secondarily impact soil respiration (Meena et al., 2020) and thus the timing of carbonate growth. In this setting, mild temperatures in December and January could drive down soil respiration, reducing soil CO₂ concentrations and favoring carbonate growth.

(2) Pedogenic carbonate that forms in late spring might not preserve as easily as earlier forming carbonate. Late spring rain events or summer monsoonal rainfall could preferentially dissolve freshly-grown carbonates and/or the outermost layers of older carbonates, leaving behind only the remnants of early, winter-grown carbonates. The mechanisms for this potential bias in dissolution remain unclear, but could relate to varying texture and/or soil depth between carbonates grown at different times of year.

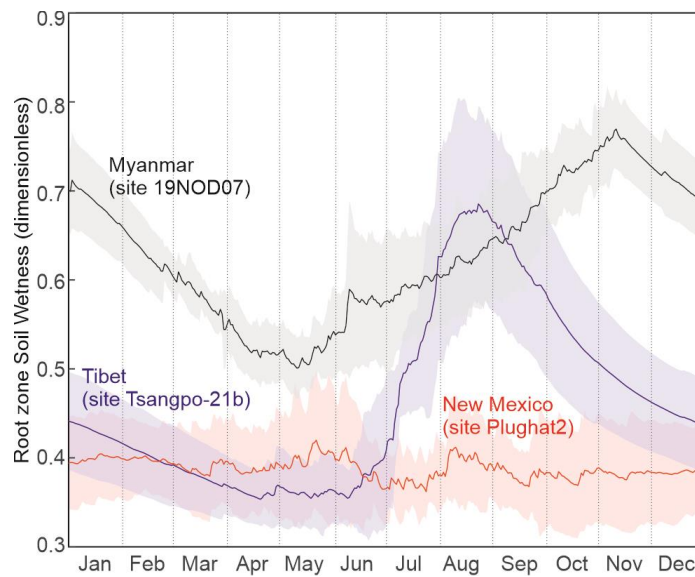


Figure 5. Root zone (0-100 cm) soil wetness from SMAP L4 satellite data (Reichle et al., 2018) at three sites with pedogenic carbonate clumped isotope data: Tsangpo-21b in Tibet (in blue; Burgener et al., 2018), Plughat-2 in New Mexico (in red; Gallagher and Sheldon, 2016), and 19NOD04 in Myanmar (in black; this study). Soil wetness unit (dimensionless) varies between 0 and 1, indicating relative saturation between completely dry conditions and completely saturated conditions, respectively; satellite data span over the 2015-2020 period and were averaged daily (curve: average; shaded area: standard deviation).

A winter bias in carbonate growth contrasts the summer bias found in Tibetan carbonates, also grown under a well-established monsoonal regime (Quade et al., 2013; Burgener et al., 2018). The soil annual hydrological budget and temperature variation in Myanmar are significantly different from those of Tibet,

341 providing potential explanations for this discrepancy. Monsoonal rainfall in Tibet is less intense (MAP
 342 commonly < 500 mm) and the rainy season is shorter. Soil wetness peaks in late summer (late August) and
 343 soils quickly dry (Fig. 5), potentially allowing carbonate to grow in early Fall. Unlike in Myanmar, where
 344 winter temperatures remain mild (CMMT > 15°C), Tibetan winter temperatures drop below freezing,
 345 drastically inhibiting evaporation and evapotranspiration and decreasing calcium activity. Soil water freezing
 346 favors cryogenic carbonate formation, which is associated with disequilibrium effects in clumped isotopic
 347 composition and commonly drives $T\Delta_{47}$ values up; the contribution of this process in Tibetan carbonates
 348 remains debated (Burgener et al., 2018). A renewal of pedogenic carbonate growth in late spring and early
 349 summer, as proposed by Quade et al. (2013), is additionally possible when soils defrost before the rainy
 350 season.

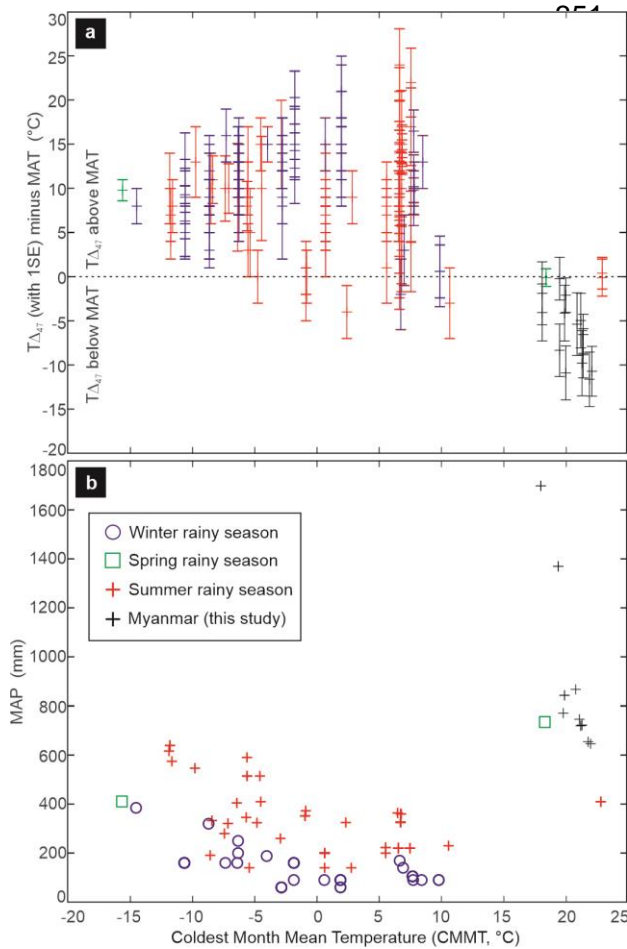


Figure 6. (a) $T\Delta_{47}$ values minus MAT of the same sites compared to their Coldest Month Mean Temperature (CMMT); $T\Delta_{47}$ error bars correspond to 1 SE. $T\Delta_{47}$ values from previous sites are from Kelson et al. (2020); CMMT, MAT, and MAP of Burmese sites from Worldclim 2.1; CMMT, MAT, and MAP from other sites from Kelson et al. (2020) or Worldclim 2.1 if not provided. (b) CMMT and MAP at the study sites (black crosses) compared to previously published soil carbonate clumped isotope data (from Kelson et al., 2020). Previously published sites are sorted according to their prominent rainy season on both panels: winter (blue crosses), spring (green crosses) and summer (red crosses); color coding is the same for both panels.

370 The apparent winter bias recorded in the Burmese
 371 pedogenic carbonates is so far unique in the clumped
 372 isotopic record of Quaternary carbonates (Fig. 6a). This is likely because the Burmese samples presented
 373 here represent an environment that is not previously addressed in clumped isotope studies, as this
 374 environment is both wetter and warmer (as demonstrated by a high CMMT; Fig 6b). Most clumped isotope
 375 data screened for robustness by Kelson et al. (2020) --more than 2 replicates, sampling depth >39 cm-- come
 376 from localities with MAP < 500 mm and more evenly distributed rainfall than the monsoonal domain,
 377 resulting in low levels of soil wetness year-round, even during the (weak) rainy season(s) (such as seen in the
 American Southwest; Fig. 5). All previous clumped isotope data sites also display cold CMMT (< 10 °C),
 which likely inhibits pedogenic carbonate growth during the cold season. Of the previously studied soil

carbonate localities, only those in Ethiopia and Kenya experience high CMMT (18-23 °C) similar to our Burmese sites (Passey et al., 2010). The Kenyan site experiences evenly distributed, moderate rainfall over the year, peaking in spring (MAP: 736 mm), while the Ethiopian localities are much drier (MAP: 410 mm) and go through two dry seasons, in winter and late spring-early summer. Both rainfall distributions likely favor multiple yearly episodes of carbonate growth. The $T\Delta_{47}$ values at both sites are in agreement with MAT (Fig. 6b), but these sites have a narrow seasonal range of temperature variation ($< \pm 4$ °C), and it is difficult to detect seasonal bias from $T\Delta_{47}$ alone.

5.3 Local parameters influencing carbonate growth and isotopic signature within the tropical domain

The spread of oxygen and carbon isotopic data among our sites suggests that multiple local factors influence carbonate growth and its isotopic signature within the Burmese lowlands.

Evaporation in soils commonly drives carbonate $\delta^{18}\text{O}$ values up and is more likely to occur under arid conditions (Cerling and Quade, 1993; Beverly et al., 2020). Spatial changes in evaporation effects have likely little impact on the spread of $\delta^{18}\text{O}$ values in our dataset, as the most depleted carbonate $\delta^{18}\text{O}$ values are only present at the drier sites of study. Interestingly, the coldest $T\Delta_{47}$ values in our Quaternary record are associated with the lowest water $\delta^{18}\text{O}$ values (-9 to -6 ‰ VSMOW; Fig. 3b), similar to rainfall $\delta^{18}\text{O}$ values reached at the end of the monsoon season (Fig. 1b), while the warmest temperatures are associated with higher $\delta^{18}\text{O}$ values (-6 to -1 ‰ VSMOW), typical of spring rainfall. These variations cannot be explained by differences in the ages of the pedogenic carbonates; carbonates grown during glacials --thus displaying the coldest temperatures-- would have higher water $\delta^{18}\text{O}$ values than carbonate grown during interglacials, as documented in Burmese speleothems (Liu et al., 2020). The entire range of modern seasonal rainfall $\delta^{18}\text{O}$ values is covered in the range of calculated soil water $\delta^{18}\text{O}$ values, suggesting the variation is due to differences in the seasonal timing of carbonate growth. Carbonates often prominently incorporate the $\delta^{18}\text{O}$ values of water that is contemporaneous with or directly preceding the period of carbonate growth rather than carry over soil water $\delta^{18}\text{O}$ values from out-of-season (Gallagher and Sheldon, 2016; Fischer-Femal and Bowen, 2021). Accordingly, the coldest $T\Delta_{47}$ values and most depleted $\delta^{18}\text{O}$ values are compatible with carbonate growth in early winter with minimum soil water storage (1-3 months), incorporating late monsoonal waters; in contrast, warmer $T\Delta_{47}$ values and higher $\delta^{18}\text{O}$ values are compatible with growth in early spring, enriched due to incorporation of spring rainwater or evaporation (Fig 3b).

Based solely on soil water $\delta^{18}\text{O}$ values, our limited dataset suggests that carbonate at drier sites (MAP <800 mm) grows preferentially in winter while growth at wetter sites (MAP >800 mm) is delayed towards early spring (Fig. 3b). The uncertainty around $T\Delta_{47}$ values remains too large to confirm that the same MAP-dependency is seen in growth temperatures. Individual carbonate nodules yield water $\delta^{18}\text{O}$ values compatible with winter and spring rain composition at the same locality, together with a wide range of $T\Delta_{47}$ values (15 ± 6 and 23 ± 4 °C 2 SE at site 19NOD06; Table 1), suggesting that MAP is not the only relevant factor impacting carbonate growth temperatures. Local (meter-scale) differences in landscape position, soil texture, or plant water use could impact soil water storage and explain some of the observed isotopic variability (Kelson et al., 2020).

The range of carbonate $\delta^{13}\text{C}$ values is particularly wide: there is an 11 ‰ difference between the most depleted samples in the wet domain and the least depleted samples in the dry domain. This difference cannot be explained by a varying amount of C4 plants, as organic matter $\delta^{13}\text{C}$ values do not show any marked contribution from C4 plants even at the driest sites (e.g. $\delta^{13}\text{C}$ always < -20 ‰ VPDB). Decreased water stress on Burmese C3 plants during glacials could potentially account for 3-5 ‰ of depletion in the pedogenic carbonates of the wetter sites (Kohn, 2010), but fails to explain the much wider range of $\delta^{13}\text{C}$ values. Seasonal variations in soil respiration rate and/or isotopic composition significantly impact soil CO_2 $\delta^{13}\text{C}$ values (Breecker et al., 2009) and could potentially explain part of this difference, as already proposed for other past monsoonal C3 records (Licht et al., 2020). Low rates and high $\delta^{13}\text{C}$ values of winter soil respiration followed by higher rates and lower $\delta^{13}\text{C}$ values of early spring respiration could partly explain the observed difference between sites on both ends of the $\delta^{13}\text{C}$ spectrum.

More generally, carbonate $\delta^{13}\text{C}$ and $\delta^{18}\text{O}$ values are not positively correlated as would be expected of arid regions, where the effects of soil evaporation and respiration are the main drivers in changing those values (Fischer-Femal and Bowen, 2020; Broz et al. 2021). We hypothesize that overall higher soil wetness year-round in central Myanmar minimizes this covariation in comparison to temperate carbonate-rich soils, while making the bulk and clumped isotope composition particularly sensitive to the seasonal rainfall distribution. Other eco-hydrological factors are likely also at play but remain to be identified with a more thorough sampling and systematic study of soil features. The soil texture, Bk horizon depth and dominant vegetation at each locality are described in Supplementary Table 1 and do not covary with bulk and clumped isotope composition (not shown). Importantly, Bk depth appears independent of local MAP, unlike observed in the temperate domain (Retallack, 2005). Our results thus highlight that carbonates grown under tropical conditions follow different growth patterns and isotope systematics than their temperate counterparts.

5.4 Implications for paleoenvironmental studies

Our dataset illustrates the high bulk and clumped isotope variability found in a limited geographical area in the tropics (ca. 10 ‰ for C and O isotopic data and 10 °C for $\text{T}\Delta_{47}$ values), driven by subtle changes in carbonate growth season influenced by local hydrological processes. This variability alone could explain a significant part of the variations found in several past bulk and clumped isotopic records without requiring dramatic changes of climate or elevation (Page et al., 2019). The processes and seasonal biases impacting carbonate growth in Myanmar today are also expected to be common in paleosols during Greenhouse intervals, which are associated with higher CMMT at mid-latitude, a wide spread of tropical ecosystems (Wing and Greenwood 1993; Toumoulin et al., 2021), and a more active hydrological cycle resulting in locally increased rainfall seasonality, as is seen in Paleogene Myanmar (Licht et al., 2014b). In particular, our results open the way for a reinterpretation of past bulk and clumped isotopic data used for the paleoaltimetry of Tibetan carbonates, which have so far systematically been interpreted as growing in summer or equally throughout the year (e.g. Botsyun et al., 2019); low stable isotopic values (< -10 ‰ VPDB) and cold $\text{T}\Delta_{47}$ values (< 25 °C) are, in this framework, considered as reflecting high elevation. While some Paleogene sites display reconstructed water $\delta^{18}\text{O}$ values that are too low (< -14 ‰ VPDB) to be solely

created by a monsoonal isotopic signature and thus require high elevations to explain them (Ingalls et al., 2020; Fang et al., 2020), others display bulk and clumped isotopic values similar to what we find today in Myanmar, and can alternatively reflect a monsoonal signature in carbonate growth at low elevation (Xiong et al., 2020). Moreover, decreasing rainfall amount and winter temperatures during gradual Tibetan uplift in the monsoonal domain should gradually move the carbonate growth season from early spring to winter, late fall, and eventually early fall and/or late spring, once the winters are too cold to favor carbonate growth and the rainy season is limited to a few months in the summer. This complex evolution makes paleoaltimetry estimates based on soil carbonate data more challenging in the monsoonal domain and for past tropical climates.

5.5 An isotopic signature for past monsoonal regimes?

While making paleoelevation estimates based solely on pedogenic carbonate bulk and clumped isotope data appears challenging, these data can provide unique insight into rainfall dynamics when MAT or elevation are independently constrained. In particular, the climatic patterns proposed as the origin of the Burmese winter bias in $T\Delta_{47}$ values, i.e. wet summers combined with dry and warm winters, are diagnostic of monsoonal areas at low altitude. Lower $T\Delta_{47}$ values than MAT should thus provide a proxy for tropical monsoonal climate. In addition, our observations suggest that C and O isotopic data could potentially provide insights into rainfall amount, though their MAP-dependency remains to be confirmed with a more systematic study of Quaternary tropical pedogenic carbonates and soil waters.

In this light, the results from the Miocene Natma Formation are meaningful and provide a proof-of-concept example for the usefulness of combined bulk and clumped isotope analysis in the tropical domain when the climate is independently constrained. Natma pedogenic carbonates yield low $T\Delta_{47}$ values (20-23 °C), high $\delta^{18}\text{O}$ (>-4 ‰ VPDB) and low $\delta^{13}\text{C}$ (<-10 ‰ VPDB) values. Following regular isotopic interpretative keys used in the temperate domain, $T\Delta_{47}$ values could be interpreted as reflecting colder summers than today's (Kelson et al., 2020), and high $\delta^{18}\text{O}$ values would reflect less monsoonal rainfall while low $\delta^{13}\text{C}$ would mean overall wetter conditions (Caves et al., 2015). These interpretations suggest a colder and wetter climate at the time of the Natma Formation, with limited monsoons and more evenly distributed rainfall over the year. They contrast with independent lines of evidence for a warmer late early to early middle Miocene globally (Steinthorsdottir et al., 2020) with intense Asian monsoons (Clift et al., 2008), and raise preservation issues, as higher but less seasonal rainfall would likely favor the dissolution of pedogenic carbonate. In contrast, fossil wood specimens of the Natma Formation reflect different ecotones of seasonal forests with coastal, mixed to dry deciduous, and wet evergreen species, suggesting a warm, seasonal monsoonal climate during the late early Miocene at least as wet as today, and possibly wetter summers (Gentis et al., 2019). In this context, low $T\Delta_{47}$ values (<25 °C) in Natma pedogenic carbonates corroborate a summer rainy season (Fig. 3b), while high $\delta^{18}\text{O}$ (>-4 ‰ VPDB) values and low $\delta^{13}\text{C}$ (<-10 ‰ VPDB) values fall on the “wet” side of the carbonate spectrum, similar to what is found today at the sampling site (Fig. 3a). This interpretation is more in line with the fossil wood assemblage, and suggests modern-like monsoonal rainfall in Myanmar in the late early Miocene. This example illustrates how different isotopic systematics are between pedogenic

carbonates in the temperate and tropical domains, and how applying inadequate interpretative keys can significantly impact paleoclimatic interpretations.

6. Conclusion

Low TA_{47} values ($<25^{\circ}\text{C}$) in Quaternary soil carbonates from central Myanmar indicate a bias in carbonate growth timing toward winter and early spring. We attribute the cold season bias to the combined effects of warm winter temperatures and intense rainfall during the summer and fall, conditions that are typical of tropical monsoonal climates. These conditions allow for carbonate growth in areas where MAP today exceeds 1700 mm. Oxygen and carbon isotopic data suggest that carbonate growth timing locally varies from early winter to early spring, with decreasing incorporation of depleted oxygen from monsoonal waters throughout the growth span. This trend is partly influenced by local MAP, with the wettest sites possibly delayed to early spring. Our results confirm that rainfall annual distribution and amount significantly impact the season of carbonate growth and its bulk and clumped isotopic record (Peters et al., 2013; Gallagher and Sheldon, 2016; Burgener et al., 2016; Kelson et al., 2020). We suggest that this expression is particularly important in tropical areas, where high soil wetness year-round makes carbonate growth more episodic and particularly sensitive to the seasonal distribution of rainfall. This sensitivity is also enhanced by high CMMT, allowing carbonate growth to move outside the warmest months of the year. This high sensitivity is expected to be more prominent in the geological record during times with higher temperatures and greater expansion of the tropical realm. “Cold” TA_{47} records in Asian paleosols, often interpreted through the lense of evolving topography, might instead provide a possible fingerprint for tropical monsoonal climate. Our understanding of pedogenic carbonate growth dynamics has been so far strongly biased toward temperate ecosystems; our results show that pedogenic carbonates grown under Burmese tropical conditions follow different dynamics and isotope systematics. These remain to be further documented and expanded to other tropical soil carbonates to gain a more complete understanding of their growth under different conditions and the resulting implications for paleoenvironmental reconstructions.

Acknowledgments

This study was financially supported by the University of Washington and European Research Council consolidator grant MAGIC 649081. We thank L. Burgener, J. Harlé, S. Shekut, C. Bourgeois, Kyi Kyi Thein, Hnin Hnin Swe, Myat Kay Thi, A. Gough, D. Perez-Pinedo, J. Westerweel, and P. Roperch for prolific discussions and assistance in the field and lab. Datasets for this research are included in the supplementary information files and archived on EarthChem (to be released upon publication).

References

Anderson, N. T., Kelson, J. R., Kele, S., Daëron, M., Bonifacie, M., Horita, J., ... & Bergmann, K. D. (2021). A unified clumped isotope thermometer calibration ($0.5\text{--}1100^{\circ}\text{C}$) using carbonate-based standardization.

- 524 *Geophysical Research Letters*, e2020GL092069.
- 525 Araguás-Araguás, L., Froehlich, K., & Rozanski, K. (1998). Stable isotope composition of precipitation over
526 southeast Asia. *Journal of Geophysical Research: Atmospheres*, 103(D22), 28721-28742.
- 527 Belousov, A., Belousova, M., Zaw, K., Streck, M. J., Bindeman, I., Meffre, S., & Vasconcelos, P. (2018).
528 Holocene eruptions of Mt. Popa, Myanmar: Volcanological evidence of the ongoing subduction of Indian
529 Plate along Arakan Trench. *Journal of Volcanology and Geothermal Research*, 360, 126-138.
- 530 Broz, A., Retallack, G. J., Maxwell, T. M., & Silva, L. C. (2021). A record of vapour pressure deficit
531 preserved in wood and soil across biomes. *Scientific reports*, 11(1), 1-12.
- 532 Bernasconi, S., Daëron, M., Bergmann, K., Bonifacie, M., Meckler, A. N., Affek, H., ... & Ziegler, M.
533 (2021). InterCarb: A community effort to improve inter-laboratory standardization of the carbonate clumped
534 isotope thermometer using carbonate standards.
- 535 Bettis III, E. A., Milius, A. K., Carpenter, S. J., Larick, R., Zaim, Y., Rizal, Y., ... & Bronto, S. (2009). Way
536 out of Africa: Early Pleistocene paleoenvironments inhabited by *Homo erectus* in Sangiran, Java. *Journal of*
537 *Human Evolution*, 56(1), 11-24.
- 538 Beverly, E., Levin, N. E., Passey, B. H., Aron, P. G., Yarian, D. A., Page, M., & Pelletier, E. M. (2020).
539 Triple oxygen and clumped isotopes in modern soil carbonate along an aridity gradient in the Serengeti,
540 Tanzania. *Earth and Space Science Open Archive ESSOAr*.
- 541 Botsyun, S., Sepulchre, P., Donnadieu, Y., Risi, C., Licht, A., & Rugenstein, J. K. C. (2019). Revised
542 paleoaltimetry data show low Tibetan Plateau elevation during the Eocene. *Science*, 363(6430).
- 543 Breecker, D. O., Sharp, Z. D., & McFadden, L. D. (2009). Seasonal bias in the formation and stable isotopic
544 composition of pedogenic carbonate in modern soils from central New Mexico, USA. *Geological Society of*
545 *America Bulletin*, 121(3-4), 630-640.
- 546 Breecker, D. O., Sharp, Z. D., & McFadden, L. D. (2010). Atmospheric CO₂ concentrations during ancient
547 greenhouse climates were similar to those predicted for AD 2100. *Proceedings of the National Academy of*
548 *Sciences*, 107(2), 576-580.
- 549 Burgener, L., Huntington, K. W., Hoke, G. D., Schauer, A., Ringham, M. C., Latorre, C., & Díaz, F. P.
550 (2016). Variations in soil carbonate formation and seasonal bias over > 4 km of relief in the western Andes
551 (30° S) revealed by clumped isotope thermometry. *Earth and Planetary Science Letters*, 441, 188-199.
- 552 Burgener, L. K., Huntington, K. W., Sletten, R., Watkins, J. M., Quade, J., & Hallet, B. (2018). Clumped
553 isotope constraints on equilibrium carbonate formation and kinetic isotope effects in freezing soils.
554 *Geochimica et Cosmochimica Acta*, 235, 402-430.

- 555 Caves, J. K., Winnick, M. J., Graham, S. A., Sjostrom, D. J., Mulch, A., & Chamberlain, C. P. (2015). Role
556 of the westerlies in Central Asia climate over the Cenozoic. *Earth and Planetary Science Letters*, 428, 33-43.
- 557 Cerling, T. E., Solomon, D. K., Quade, J. A. Y., & Bowman, J. R. (1991). On the isotopic composition of
558 carbon in soil carbon dioxide. *Geochimica et Cosmochimica Acta*, 55(11), 3403-3405.
- 559 Clift, P. D., Hodges, K. V., Heslop, D., Hannigan, R., Van Long, H., & Calves, G. (2008). Correlation of
560 Himalayan exhumation rates and Asian monsoon intensity. *Nature geoscience*, 1(12), 875-880.
- 561 Colin, C., Bertaux, J., Turpin, L., & Kissel, C. (2001). Dynamique de l'érosion dans le bassin versant de
562 l'Irrawaddy au cours des deux derniers cycles climatiques (280–0 ka). *Comptes Rendus de l'Académie des
563 Sciences-Series IIA-Earth and Planetary Science*, 332(8), 483-489.
- 564 DiNezio, P. N., Tierney, J. E., Otto-Bliesner, B. L., Timmermann, A., Bhattacharya, T., Rosenbloom, N., &
565 Brady, E. (2018). Glacial changes in tropical climate amplified by the Indian Ocean. *Science advances*,
566 4(12), eaat9658.
- 567 Ehleringer, J. R., Lin, Z. F., Field, C. B., Sun, G. C., & Kuo, C. Y. (1987). Leaf carbon isotope ratios of
568 plants from a subtropical monsoon forest. *Oecologia*, 72(1), 109-114.
- 569 Fang, X., Dupont-Nivet, G., Wang, C., Song, C., Meng, Q., Zhang, W., ... & Chen, Y. (2020). Revised
570 chronology of central Tibet uplift (Lunpola Basin). *Science Advances*, 6(50), eaba7298.
- 571 Fick, S. E., & Hijmans, R. J. (2017). WorldClim 2: new 1-km spatial resolution climate surfaces for global
572 land areas. *International journal of climatology*, 37(12), 4302-4315.
- 573 Fischer-Femal, B. J., & Bowen, G. J. (2021). Coupled carbon and oxygen isotope model for pedogenic
574 carbonates. *Geochimica et Cosmochimica Acta*, 294, 126-144.
- 575 Gallagher, T. M., & Sheldon, N. D. (2016). Combining soil water balance and clumped isotopes to
576 understand the nature and timing of pedogenic carbonate formation. *Chemical Geology*, 435, 79-91.
- 577 Gallagher, T. M., Hren, M., & Sheldon, N. D. (2019). The effect of soil temperature seasonality on climate
578 reconstructions from paleosols. *American Journal of Science*, 319(7), 549-581.
- 579 Gentis, N., Boura, A., & De Franceschi, D. (2019). Fossil wood from the Miocene of Myanmar: application
580 to the reconstruction of monsoonal paleoenvironments. *Congrès Agora paleobotanica*, Jul 2019, Lille,
581 France. [note: a scientific paper based on this conference talk is in review at *Geodiversitas* and available on
582 ESSOAR: <https://www.essoar.org/doi/abs/10.1002/essoar.10506983.1>].
- 583 Hanpattanakit, P., Leclerc, M. Y., Mcmillan, A. M., Limtong, P., Maeght, J. L., Panuthai, S., ... &
584 Chidthaisong, A. (2015). Multiple timescale variations and controls of soil respiration in a tropical dry
585 dipterocarp forest, western Thailand. *Plant and soil*, 390(1), 167-181.

- 586 Hoke, G. D., Liu-Zeng, J., Hren, M. T., Wissink, G. K., & Garziona, C. N. (2014). Stable isotopes reveal
587 high southeast Tibetan Plateau margin since the Paleogene. *Earth and Planetary Science Letters*, 394, 270-
588 278.
- 589 Huth, T. E., Cerling, T. E., Marchetti, D. W., Bowling, D. R., Ellwein, A. L., & Passey, B. H. (2019).
590 Seasonal bias in soil carbonate formation and its implications for interpreting high-resolution paleoarchives:
591 Evidence from southern Utah. *Journal of Geophysical Research: Biogeosciences*, 124(3), 616-632.
- 592 Ingalls, M., Rowley, D., Olack, G., Currie, B., Li, S., Schmidt, J., ... & Colman, A. (2018). Paleocene to
593 Pliocene low-latitude, high-elevation basins of southern Tibet: Implications for tectonic models of India-Asia
594 collision, Cenozoic climate, and geochemical weathering. *GSA Bulletin*, 130(1-2), 307-330.
- 595 Kelson, J. R., Huntington, K. W., Schauer, A. J., Saenger, C., & Lechler, A. R. (2017). Toward a universal
596 carbonate clumped isotope calibration: Diverse synthesis and preparatory methods suggest a single
597 temperature relationship. *Geochimica et Cosmochimica Acta*, 197, 104-131.
- 598 Kelson, J. R., Huntington, K. W., Breecker, D. O., Burgener, L. K., Gallagher, T. M., Hoke, G. D., &
599 Petersen, S. V. (2020). A proxy for all seasons? A synthesis of clumped isotope data from Holocene soil
600 carbonates. *Quaternary Science Reviews*, 234, 106259.
- 601 Khaing, T. T., Pasion, B. O., Lapuz, R. S., & Tomlinson, K. W. (2019). Determinants of composition,
602 diversity and structure in a seasonally dry forest in Myanmar. *Global Ecology and Conservation*, 19, e00669.
- 603 Kim, S. T., & O'Neil, J. R. (1997). Equilibrium and nonequilibrium oxygen isotope effects in synthetic
604 carbonates. *Geochimica et cosmochimica acta*, 61(16), 3461-3475.
- 605 Kohn, M. J. (2010). Carbon isotope compositions of terrestrial C3 plants as indicators of (paleo) ecology and
606 (paleo) climate. *Proceedings of the National Academy of Sciences*, 107(46), 19691-19695.
- 607 Kume, T., Tanaka, N., Yoshifuji, N., Chatchai, T., Igarashi, Y., Suzuki, M., & Hashimoto, S. (2013). Soil
608 respiration in response to year-to-year variations in rainfall in a tropical seasonal forest in northern Thailand.
609 *Ecohydrology*, 6(1), 134-141.
- 610 Lai Lai Aung, Ei Ei Zin, Pwint Theingi, Naw Elvera, Phyu Phyu Aung, Thu Thu Han, Yamon Oo, &
611 Skaland R.G. (2017). Myanmar Climate Report, *MET Report* No. 9/2017.
- 612 Licht, A., Cojan, I., Caner, L., Soe, A. N., Jaeger, J. J., & France-Lanord, C. (2014). Role of permeability
613 barriers in alluvial hydromorphic palaeosols: the Eocene Pondaung Formation, Myanmar. *Sedimentology*,
614 61(2), 362-382.
- 615 Licht, A., Van Cappelle, M., Abels, H. A., Ladant, J. B., Trabucho-Alexandre, J., France-Lanord, C., ... &
616 Terry Jr, D. (2014b). Asian monsoons in a late Eocene greenhouse world. *Nature* 513, 501-506.

- 617 Licht, A., Dupont-Nivet, G., Meijer, N., Rugenstein, J. C., Schauer, A., Fiebig, J., ... & Guo, Z. (2020).
618 Decline of soil respiration in northeastern Tibet through the transition into the Oligocene icehouse.
619 *Palaeogeography, Palaeoclimatology, Palaeoecology*, 560, 110016.
- 620 Liu, G., Li, X., Chiang, H. W., Cheng, H., Yuan, S., Chawchai, S., ... & Wang, X. (2020). On the glacial-
621 interglacial variability of the Asian monsoon in speleothem $\delta^{18}\text{O}$ records. *Science advances*, 6(7), eaay8189.
- 622 Meena, A., Hanief, M., Dinakaran, J., & Rao, K. S. (2020). Soil moisture controls the spatio-temporal pattern
623 of soil respiration under different land use systems in a semi-arid ecosystem of Delhi, India. *Ecological*
624 *Processes*, 9(1), 1-13.
- 625 Montanez, I. P. (2013). Modern soil system constraints on reconstructing deep-time atmospheric CO_2 .
626 *Geochimica et Cosmochimica Acta*, 101, 57-75.
- 627 Page, M., Licht, A., Dupont-Nivet, G., Meijer, N., Barbolini, N., Hoorn, C., ... & Guo, Z. (2019).
628 Synchronous cooling and decline in monsoonal rainfall in northeastern Tibet during the fall into the
629 Oligocene icehouse. *Geology*, 47(3), 203-206.
- 630 Peters, N. A., Huntington, K. W., & Hoke, G. D. (2013). Hot or not? Impact of seasonally variable soil
631 carbonate formation on paleotemperature and O-isotope records from clumped isotope thermometry. *Earth*
632 *and Planetary Science Letters*, 361, 208-218.
- 633 Pivnik, D. A., Nahm, J., Tucker, R. S., Smith, G. O., Nyein, K., Nyunt, M., & Maung, P. H. (1998).
634 Polyphase deformation in a fore-arc/back-arc basin, Salin subbasin, Myanmar (Burma). *AAPG bulletin*,
635 82(10), 1837-1856.
- 636 Quade, J., Breecker, D. O., Daëron, M., & Eiler, J. (2011). The paleoaltimetry of Tibet: An isotopic
637 perspective. *American Journal of Science*, 311(2), 77-115.
- 638 Quade, J., Eiler, J., Daeron, M., & Achyuthan, H. (2013). The clumped isotope geothermometer in soil and
639 paleosol carbonate. *Geochimica et Cosmochimica Acta*, 105, 92-107.
- 640 Railsback, L. B. (2021). Pedogenic carbonate nodules from a forested region of humid climate in central
641 Tennessee, USA, and their implications for interpretation of C_3 - C_4 relationships and seasonality of meteoric
642 precipitation from carbon isotope ($\delta^{13}\text{C}$) data. *CATENA*, 200, 105169.
- 643 Reichle, R., G. De Lannoy, R. D. Koster, W. T. Crow, J. S. Kimball, and Q. Liu. 2018. SMAP L4 Global 3-
644 hourly 9 km EASE-Grid Surface and Root Zone Soil Moisture Analysis Update, Version 4. Boulder,
645 Colorado USA. *NASA National Snow and Ice Data Center Distributed Active Archive Center*.
646 <https://doi.org/10.5067/60HB8VIP2T8W>. [Date Accessed].
- 647 Retallack, G. J. (2005). Pedogenic carbonate proxies for amount and seasonality of precipitation in paleosols.

- 648 *Geology*, 33(4), 333-336.
- 649 Romanek, C. S., Grossman, E. L., & Morse, J. W. (1992). Carbon isotopic fractionation in synthetic
650 aragonite and calcite: effects of temperature and precipitation rate. *Geochimica et cosmochimica acta*, 56(1),
651 419-430.
- 652 Rubio, V. E., & Detto, M. (2017). Spatiotemporal variability of soil respiration in a seasonal tropical forest.
653 *Ecology and evolution*, 7(17), 7104-7116.
- 654 Saraswat, R., Lea, D. W., Nigam, R., Mackensen, A., & Naik, D. K. (2013). Deglaciation in the tropical
655 Indian Ocean driven by interplay between the regional monsoon and global teleconnections. *Earth and*
656 *Planetary Science Letters*, 375, 166-175.
- 657 Singh, L., & Singh, S. (1972). Chemical and morphological composition of kankar nodules in soils of the
658 Vindhyan region of Mirzapur, India. *Geoderma*, 7(3-4), 269-276.
- 659 Stamp, L. D. (1940). The Irrawaddy River. *The Geographical Journal*, 95(5), 329-352.
- 660 Steinhorsdottir, M., Coxall, H. K., de Boer, A. M., Huber, M., Barbolini, N., Bradshaw, C. D., ... &
661 Strömberg, C. A. E. (2020). The Miocene: the Future of the Past. *Paleoceanography and Paleoclimatology*,
662 e2020PA004037.
- 663 Toumoulin, A., Tardif, D., Donnadiou, Y., Licht, A., Ladant, J. B., Kunzmann, L., & Dupont-Nivet, G.
664 (2021). Evolution of continental temperature seasonality from the Eocene greenhouse to the Oligocene
665 icehouse-A model-data comparison. *Climate of the Past Discussions*, 1-30. ([https://doi.org/10.5194/cp-2021-](https://doi.org/10.5194/cp-2021-27)
666 27)
- 667 Van Der Kaars, S., & Dam, R. (1997). Vegetation and climate change in West-Java, Indonesia during the last
668 135,000 years. *Quaternary International*, 37, 67-71.
- 669 Westerweel, J., Licht, A., Cogné, N., Roperch, P., Dupont-Nivet, G., Kay Thi, M., ... & Wa Aung, D. (2020).
670 Burma Terrane collision and northward indentation in the Eastern Himalayas recorded in the Eocene-
671 Miocene Chindwin Basin (Myanmar). *Tectonics*, 39(10), e2020TC006413.
- 672 Xiong, Z., Ding, L., Spicer, R. A., Farnsworth, A., Wang, X., Valdes, P. J., ... & Yue, Y. (2020). The early
673 Eocene rise of the Gonjo Basin, SE Tibet: From low desert to high forest. *Earth and Planetary Science*
674 *Letters*, 543, 116312.

Localities			Climate parameters from WorldClim V2, res: 5min				Clumped isotopic data									
age	location on fig. 1	name	MAT (in °C)	WMMT (in °C)	CMMT (in °C)	MAP (in mm)	<i>n</i>	Carbonate δ ¹³ C (‰ VPDB)	δ ¹³ C S.E. (‰ VPDB)	Carbonate δ ¹⁸ O (‰ VPDB)	δ ¹⁸ O S.E. (‰ VPDB)	Δ ₄₇ Intercarb acid (‰)	Δ ₄₇ S.E. (‰)	TΔ ₄₇ (°C)	TΔ ₄₇ S.E. (°C)	Soil Water δ ¹⁸ O (‰ VSMOW)
Quaternary soils	1	17NOD01	27.2	31.3	21.2	747	8	-6.08	0.02	-4.56	0.16	0.6904	0.0092	22.1	3.0	-2.8
	2	17NOD04	25.1	29.6	19.9	772	11	-6.97	0.04	-10.11	0.02	0.6943	0.0099	20.9	3.2	-8.6
	3	19NOD02	24.3	28.5	18.1	1701	6	-10.18	0.02	-4.39	0.03	0.6898	0.0107	22.3	3.5	-2.6
	3	19NOD03	24.3	28.5	18.1	1701	7	-10.16	0.03	-6.71	0.07	0.6965	0.0099	20.2	3.1	-5.3
	4	19NOD04	25.7	29.8	19.5	1372	9	-14.72	0.01	-4.07	0.03	0.7056	0.0097	17.3	3.0	-3.3
							4	-13.92	0.01	-4.00	0.02	0.6806	0.0073	25.4	2.4	-1.5
	5	19NOD06	25.7	30.0	20.0	845	7	-8.44	0.02	-7.44	0.03	0.7140	0.0099	14.7	3.0	-7.2
							6	-8.33	0.01	-6.63	0.07	0.6862	0.0059	23.5	2.0	-4.6
	6	19NOD07	27.6	31.9	22.1	647	10	-6.97	0.01	-6.85	0.03	0.7072	0.0092	16.8	2.8	-6.2
	5	19NOD08	27	31.3	21.3	720	10	-6.48	0.02	-8.86	0.13	0.7061	0.0121	17.1	3.7	-8.1
	7	19NOD09	27.3	31.6	21.9	655	7	-7.57	0.06	-7.36	0.07	0.7111	0.0099	15.6	3.0	-7.0
	8	20NOD01	27	31.5	20.9	869	7	-7.70	0.09	-5.43	0.07	0.0096	0.0099	22.2	3.2	-3.6
	9	20NOD03	26.8	31.0	21.4	723	8	-9.89	0.02	-8.59	0.06	0.7063	0.0093	17.1	2.9	-7.9
							4	-9.19	0.01	-7.07	0.03	0.6965	0.0073	20.2	2.3	-5.7
Early Miocene	3	19NAT13	N/A				8	-9.70	0.48	-4.13	0.90	0.6976	0.0121	19.8	3.8	-2.8
	3	19NAT01	N/A				5	-9.91	0.06	-1.63	0.05	0.6881	0.0091	22.9	3.0	0.3

Figure 6.

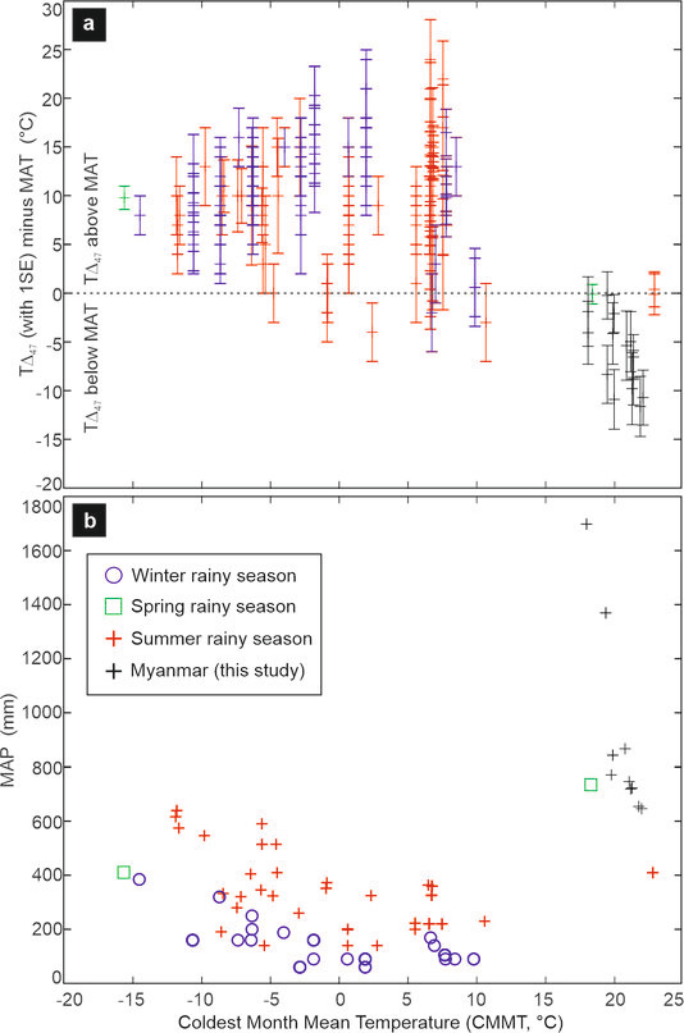


Figure 2.

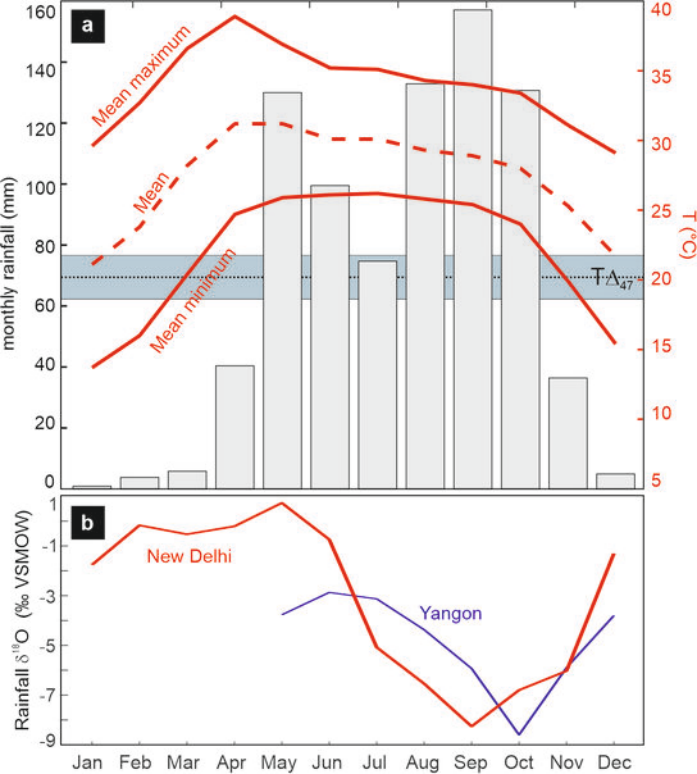


Figure 1.

- + Climate station
- 200 mm isohyets
- Late Quaternary soil samples
- Early Miocene paleosols



Figure 5.

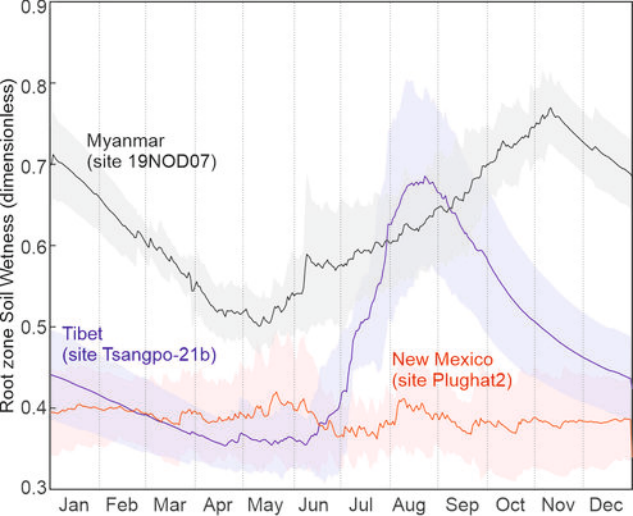


Figure 4.

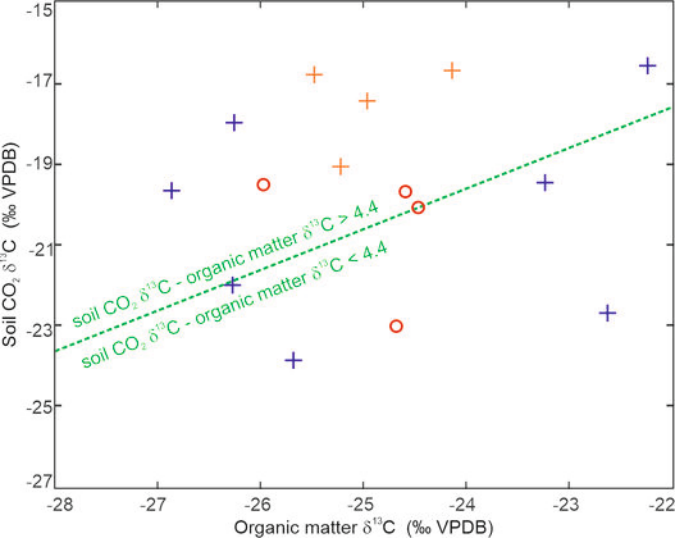


Figure 3.

